Characterization of Metamaterials Using a Strip Line Fixture

Leila Yousefi, *Member, IEEE*, Muhammed Said Boybay, *Member, IEEE*, and Omar M. Ramahi, *Fellow, IEEE*

***Abstract*—A method is introduced to measure the effective constitutive parameters of metamaterials having negative permittivity, negative permeability, or negative permeability and negative permittivity simultaneously. The method is based on the strip line topology, thus offering low cost and low setup complexity in comparison to other methods. The method proposed here is validated by numerically simulating the measurement setup while using different types of metamaterials. To validate the method experimentally, a metamaterial having negative permeability over a band of frequencies is characterized. Good agreement is obtained between the experimental and numerical results.**

***Index Terms*—Artificial magnetic materials, characterization, fractal Hilbert curves, metamaterials, permeability, permittivity, strip line fixture.**

I. Introduction

METAMATERIALS are artificial materials engineered for specific electric and magnetic responses [1]–[5]. Since the first attempts for designing metamaterials [6], [7], new applications of such materials have been proposed. In addition to the extraordinary properties and applications of metmaterials such as superlensing [5] and cloaking [8]; applications related to antenna technologies [9]–[12], near field characterization methods [13] and sub-wavelength resonators [14], have been reported. In order to efficiently realize these applications, new metamaterial designs have been proposed to increase the bandwidth and reduce the loss or the size of the unit cell [15]–[18].

Characterization of the electric and magnetic properties of metamaterials is crucial in the design and fabrication cycle. For design verification, the electrical and magnetic properties of the structure need to be measured. Since metamaterials are typically inhomogeneous and anisotropic (except for some designs as in [19], [20]), their characterization presents several challenges. Several experimental methods have been reported for retrieval of the constitutive parameters of metamaterials such as the resonator method [21], [22], the free-space method [23]–[25], the waveguide method [26], [27], and the microstrip line method [28]. Each of these methods has its advantages and disadvantages [29].

The resonator method provides high accuracy but it is inherently narrowband, and an individual measurement setup should be prepared for retrieval of the constitutive parameter at each single frequency; therefore, it is not a good candidate for characterization of metamaterials which are dispersive in nature. The free-space approach, on the other hand, provides good accuracy, however, at the cost of an expensive setup that involves two horn antennas combined with lens assemblies to generate plane waves [24]. Furthermore, in the free-space method, since standard horn antennas have limited frequency bandwidth, different setups are needed to test metamaterials operating at different frequency bands (for example, an antenna used for testing a structure which operates at 2 GHz cannot be used to test another structure which operates at 3 GHz). In the waveguide method, the sample of the metamaterial is placed at the cross section of a waveguide and its constitutive parameters are calculated from the reflected and transmitted waves [26], [27]. The setup needed for this method is less costly when compared to the free-space method, but to test metamaterials operating at different frequency bands, different setups are needed (a disadvantage shared with the free-space method). Another severe constraint on the waveguide method is that a large metamaterial sample is required to fill the entire cross section of the waveguide. This would be costly when testing metamaterials that operate at lower microwave frequencies, (as an example, to test a metamaterial operating at 500 MHz, the sample size would be approximately 0.5 m $\times$ 0.2 m).

The microstrip line method which was reported in [28], [30] has the advantage of lower cost setup in comparison to the free-space or the waveguide methods, while having the capability to extract the permeability and permittivity over a wide band of frequencies (in comparison to the resonator method). However, since the microstrip line method supports quasi-TEM mode, approximate equations based on conformal mapping techniques are required for calculation of its characteristic impedance. As shown in [30], these approximate formulas impose restrictions when extracting negative permittivity or permeability values.

In this paper, a new method based on strip line topology is presented for characterization of metamaterials. The proposed method is suitable for characterization of all types of metamaterial structures including single negative and double negative media. Comparing this method to the free-space method [23]–[25], the method presented here has the advantages of smaller sample size and inexpensive setup requirement. Unlike the free-space method which needs an expensive setup of two horn antennas combined with lens assemblies, the strip line setup is simple and inexpensive. In this method a small sample

Manuscript received March 30, 2010; revised August 05, 2010; accepted September 27, 2010. Date of publication January 28, 2011; date of current version April 06, 2011.

The authors are with the Electrical and Computer Engineering Department, University of Waterloo, Waterloo ON N2L 3G1, Canada (e-mail: lyousefi@uwaterloo.ca; msboybay@uwaterloo.ca; oramahi@ece.uwaterloo.ca).

Color versions of one or more of the figures in this paper are available online at http://ieeexplore.ieee.org.

Digital Object Identifier 10.1109/TAP.2011.2109360

of the metamaterial is required, while the free-space approach needs a sample of the size of several wavelengths [23]–[25] to be able to perform plane wave measurement.

In comparison with the rectangular waveguide method [26], [27], the method presented here has the advantages of smaller sample size requirement, inexpensive setup, and the capability of TEM mode excitation. In the waveguide method, the TEM mode is not supported leading to a non-uniform field in the cross section, which consequently complicates the retrieval process [26], [27]. In the rectangular waveguide method, the size of the metamaterial sample should be at least half of the wavelength at the resonant frequency due to the cutoff frequency restriction. Additionally, the rectangular waveguide method requires standard coaxial to waveguide adaptors which add to the setup cost and complexity. The parallel plate waveguide method [31] supports the TEM mode and therefore provides more flexibility in the sample size and easier retrieval process when compared to the rectangular waveguide method. However; to be able to excite a parallel plate waveguide with coaxial ports, a precise tapering is required [31] which makes fabrication of the setup both complex and expensive.

In comparison to the microstrip line method, the method presented here has the advantage of supporting a TEM mode which avoids restrictions introduced by the quasi-TEM nature of the fields in the microstrip line setup [30].

Various microstrip and strip line-based retrieval methods with different configurations were reported in the literature for characterization of natural materials [32]–[39], but to the authors' knowledge, no strip line-based method is reported for characterization of metamaterials which are typically anisotropic and dispersive.

In the following sections, first the retrieval method is explained. Then in Section III, using numerical full wave analysis, the accuracy of the method is verified for various types of metamaterials. Finally in Section IV, the method is used for experimental characterization of magnetic metamaterials with unit cells of 3rd order fractal Hilbert configuration.

II. Retrieval Method

The setup configuration is shown in Fig. 1. The setup consists of a two-port strip line fixture. The substrate of the strip line includes three parts: two double positive dielectric with known constitutive parameters at sides next to the excitation ports, and the metamaterial to be characterized placed in the middle. By measuring the scattering parameters of this two-port strip line fixture, the permittivity and permeability of the metamaterial under test are extracted. Based on the coordinate system presented in Fig. 1, the y component of the magnetic field and the x component of the electric field are the dominant field components in the strip line structure. Therefore this configuration can be used for retrieval of μ_y and ϵ_x.

The method used here shares the theoretical foundation with the free-space approach [23]–[25] in the sense that the two methods use reflection and transmission of waves from the metamaterial sample to extract the constitutive parameters. However, as explained in the introduction section, the method presented here has several benefits over the free-space method from the fabrication and measurement point of view.

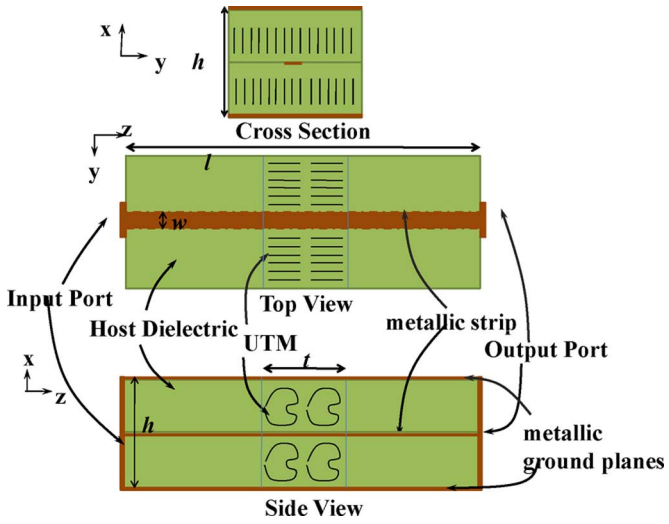

Fig. 1. The setup configuration for the strip line fixture used for extraction of the permittivity and permeability of the metamaterial media.

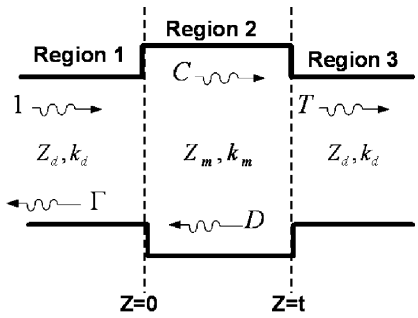

Fig. 2. Transmission line model of the setup configuration shown in Fig. 1.

The transmission line model shown in Fig. 2 is used to analyze the behavior of the field in the substrate. In this model, three transmission lines are used to represent the three regions of the strip line fixture shown in Fig. 1. According to this model, the voltage and current in all three regions are formulated by

$$\text{Region I}: V_I = e^{-jk_d z} + \Gamma e^{+jk_d z} \tag{1}$$

$$I_I = \frac{1}{Z_d}\left(e^{-jk_d z} - \Gamma e^{+jk_d z}\right) \tag{2}$$

$$\text{Region II}: V_{II} = Ce^{-jk_m z} + De^{+jk_m z} \tag{3}$$

$$I_{II} = \frac{1}{Z_m}\left(Ce^{-jk_m z} - De^{+jk_m z}\right) \tag{4}$$

$$\text{Region III}: V_{III} = Te^{-jk_d (z-t)} \tag{5}$$

$$I_{III} = \frac{T}{Z_d} e^{-jk_d (z-t)} \tag{6}$$

where k_d and Z_d are the propagation constant and characteristic impedance in the known dielectric (Regions I, and III in Fig. 2), respectively. Since the known dielectric is nonmagnetic and isotropic, k_d and Z_d can be written as [40]

$$k_d = \omega\sqrt{\epsilon_0 \epsilon_d \mu_0} \tag{7}$$

$$Z_d = 30\pi\sqrt{\frac{\mu_0}{\epsilon_0 \epsilon_d}}\left[\frac{h}{W_e + 0.441h}\right] \tag{8}$$

$$W_e = \begin{cases} W & \frac{W}{h} > 0.35 \\ W - h\left(0.35 - \frac{W}{h}\right)^2 & \frac{W}{h} < 0.35 \end{cases} \tag{9}$$

where W is the width of the strip line, h is the total height of the substrate and ϵ_d is the relative permittivity of the known dielectric. In (3) and (4), k_m and Z_m are the propagation constant and characteristic impedance in the unknown metamaterial sample, respectively. Since the metamaterial sample is in general anisotropic, the direction of the $\mathbf{E}$ and $\mathbf{H}$ fields should be considered when deriving k_m, and Z_m. In the stripline topology shown in Fig. 1 the dominant $\mathbf{E}$ component is in the x direction and the dominant $\mathbf{H}$ component is in the y direction. Therefore k_m, and Z_m are formulated as

$$k_m = \omega\sqrt{\epsilon_0\mu_0\epsilon_x\mu_y} \tag{10}$$

$$Z_m = 30\pi\sqrt{\frac{\mu_0\mu_y}{\epsilon_0\epsilon_x}}\left[\frac{h}{W_e + 0.441h}\right] \tag{11}$$

$$W_e = \begin{cases} W & \frac{W}{h} > 0.35 \\ W - h\left(0.35 - \frac{W}{h}\right)^2 & \frac{W}{h} < 0.35 \end{cases} \tag{12}$$

where μ_y is the permeability in the y direction, and ϵ_x is the permittivity in the x direction. In order to express the permittivity and permeability of the metamaterial in terms of the measured S-parameters, (1)–(6) are solved by applying the boundary conditions at $z = 0$ and $z = t$ yielding the following relationships:

$$\mu_y = \frac{Z_m k_m}{Z_d k_d}, \epsilon_x = \frac{\epsilon_d k_m Z_d}{Z_m k_d} \tag{13}$$

$$Z_m = \pm Z_d\sqrt{\frac{(1+\Gamma)^2 - T^2 e^{-j2k_d t}}{(1-\Gamma)^2 - T^2 e^{-j2k_d t}}} \tag{14}$$

$$\Gamma = S_{11}e^{-j2k_d d}, T = S_{21}e^{-j2k_d d} \tag{15}$$

$$e^{-jk_m t} = X \pm j\sqrt{1 - X^2} \tag{16}$$

$$X = \frac{1 - \Gamma^2 + T^2 e^{-j2k_d t}}{2Te^{-jk_d t}}. \tag{17}$$

The formulas presented for Z_m (11) and Z_d (8) are approximate [40]. Notice that the bracketed expressions in (11) and (8) are identical since the width of the strip line W and the height of the substrate h are the same for the dielectric part and metamaterial part. Therefore, when calculating the extracted parameters, μ_y and ϵ_x, the bracketed parts of the expressions in Z_m and Z_d, cancel out. As a result, the approximations embedded in Z_m and Z_d that relate to the line width and substrate height will not affect the extracted parameters μ_y, ϵ_x, and thus, the accuracy of the method.

In the above equations, only the dominant electric and magnetic fields are considered. However, in the strip line structure, the y component of $\mathbf{E}$ as well as the x component of $\mathbf{H}$ which are ignored in (10) and (11) are present in the field distribution. In the case of isotropic sample, the fact that the permittivity and permeability are the same in all the directions does not affect the accuracy of the results. However, in the case of anisotropic metamaterials, neglecting the non-dominant field components is expected to affect the accuracy of the extracted permittivity and permeability. In Section III, using full wave numerical analysis, the effect of anisotropy is investigated and a solution is proposed.

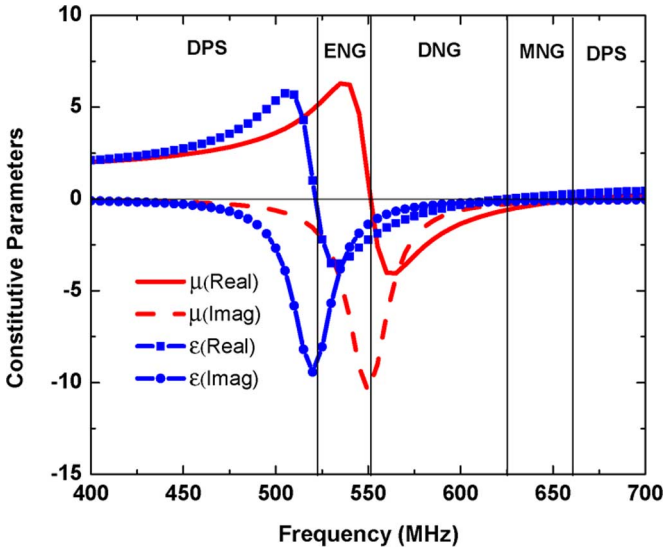

Fig. 3. The constitutive parameters of the sample under test (Frequency-dependent case).

III. Full Wave Numerical Analysis

To investigate the accuracy of the method and to analyze the effect of having anisotropic samples, full wave numerical simulation is used. Ansoft HFSS10, a commercial simulation tool based on the three-dimensional finite element method, is used for numerical analysis.

A. Isotropic Metamaterial Sample

To test the method for metamaterial samples with frequency-dependent constitutive parameters, a metamaterial with constitutive parameters shown in Fig. 3 is used as the sample under test. In this section, we assume that the sample is isotropic. In the next section we consider anisotropic samples. The parameters shown in Fig. 3 is generated using the Lorentz model [41] for both permittivity and permeability

$$\epsilon_r = 1 + \frac{f_{pe}^2}{f_{0e}^2 - f^2 + jG_e f} \tag{18}$$

$$\mu_r = 1 + \frac{f_{pm}^2}{f_{0m}^2 - f^2 + jG_m f} \tag{19}$$

where the parameters in the above equations are selected as: $f_{pe} = 350$ MHz, $f_{pm} = 380$ MHz, $f_{0e} = 520$ MHz, $f_{0m} = 550$ MHz, and $G_e = G_m = 25$ MHz.

The constitutive parameters data shown in Fig. 3 includes all possible cases: double positive, ϵ-negative, μ-negative, and double negative. Therefore; by characterizing this sample, the accuracy of method will be tested for all types of metamaterials. Using numerical simulations, the S-parameters are generated for the test material, and using (13)–(17), the constitutive parameters are calculated. In Figs. 4 and 5, the superimposed plots of the extracted parameters and the actual assigned parameters are presented. A strong agreement is observed between the extracted parameters and the actual data. In this simulation, parameters of the strip line fixture (see Fig. 1) are chosen as follows: $l = 23$ cm, $t = 2$ cm, $h = 22$ mm, $W = 18$ mm, the host dielectric is Rogers RT/duroid 5880 with $\epsilon_d = 2.2$, and $\tan\delta = 0.0009$.

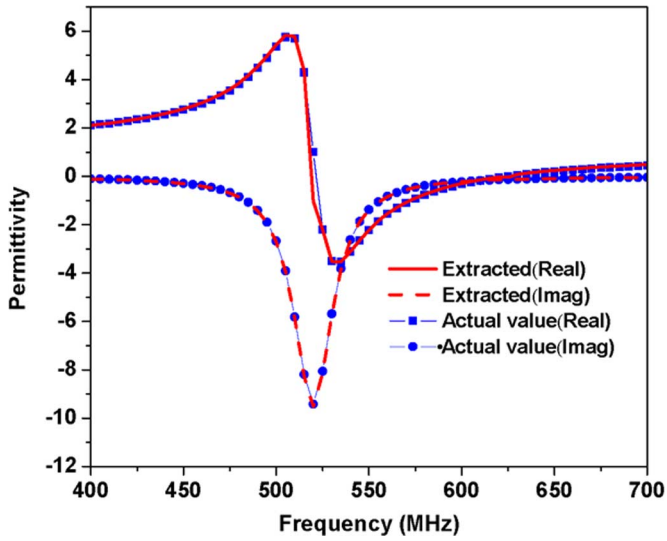

Fig. 4. Extracted permittivity for the data shown in Fig. 3.

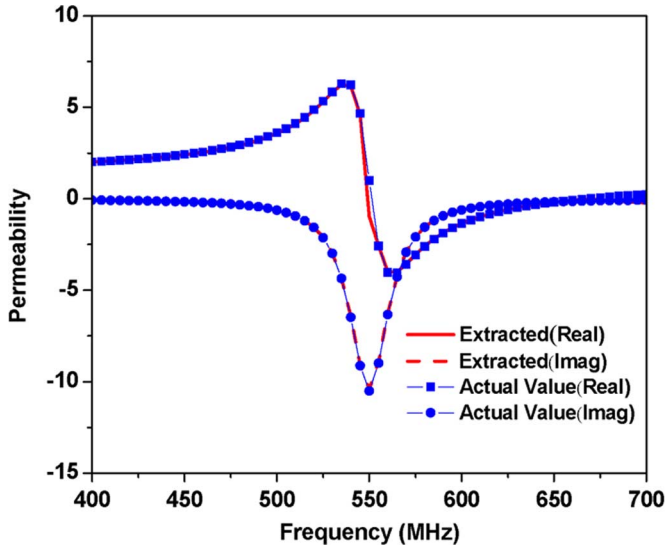

Fig. 5. Extracted permeability for the data shown in Fig. 3.

B. Anisotropic Metamaterial Sample and Curve Fitting

Usually metamaterial designs and applications involve anisotropy in the structure. Therefore characterization of anisotropic samples using the proposed method has a practical importance. The equations used for extraction of permittivity and permeability from S_{21} and S_{11} are derived by neglecting the effect of non-dominant field components on the characteristic impedance and propagation constant. Therefore, we expect some deviation between the extracted parameters and the actual parameters when the sample is anisotropic. To present a quantitative study on this deviation, we assume a sample with the following permittivity and permeability tensors:

$$\epsilon = \epsilon_0 \begin{pmatrix} \epsilon_x & 0 & 0 \\ 0 & 2.2 & 0 \\ 0 & 0 & \epsilon_z \end{pmatrix} \tag{20}$$

$$\mu = \mu_0 \begin{pmatrix} 1 & 0 & 0 \\ 0 & \mu_y & 0 \\ 0 & 0 & 1 \end{pmatrix}. \tag{21}$$

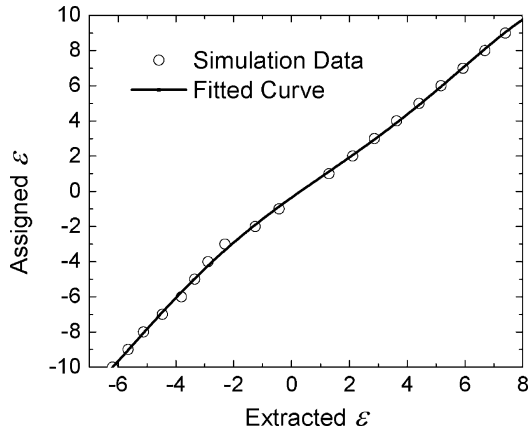

Fig. 6. Results of simulation for anisotropic sample. Extracted permittivity (ϵ_e) is plotted versus actual value of permittivity (ϵ_x).

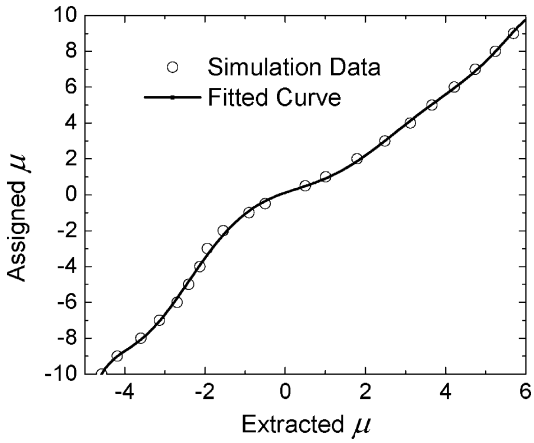

Fig. 7. Results of simulation for anisotropic sample. Extracted permeability (μ_e) is plotted versus actual value of permeability (μ_y).

First we assume a frequency-independent sample with constant values for $\epsilon_x = \epsilon_z$ and μ_y. Using the extraction procedure used in Section III.A, the constitutive parameters are calculated. In Figs. 6 and 7, assigned values of constitutive parameters are plotted as a function of extracted values. In this simulation, the topological dimensions of the strip line fixture and the host dielectric are as in Section III.A.

The results presented in Figs. 6 and 7 show that the extracted values μ_e and ϵ_e are not equal to the assigned values μ_y and ϵ_x. Notice that if the extracted and assigned values were equal, the two curves in Figs. 6 and 7 would be straight lines with unity slope. The reason behind this deviation for the anisotropic samples, as explained in Section II, is due to neglecting the non-dominant components of $\mathbf{E}$ and $\mathbf{H}$ when deriving (10)–(17). In order to address this problem, we propose a post-processing solution to compensate for the effect of anisotropy. In this solution, first we obtain a function to describe the relation between the extracted and assigned parameters. Then, we apply the derived function to the measurement results to compensate the effect of anisotropy. Using curve fitting tools in MATLAB, polynomial functions that represent the numerical results presented in

Figs. 6 and 7 are derived. The fitted functions are also plotted in Figs. 6 and 7. The formulas of the resultant polynomials are

$$\begin{aligned}\mu_y = &-3.93\times10^{-5}\mu_e^8 + 3.2\times10^{-4}\mu_e^7 \\ &+ 1.4\times10^{-3}\mu_e^6 \\ &- 0.0146\mu_e^5 - 6.6\times10^{-3}\mu_e^4 + 0.215\mu_e^3 \\ &- 0.19\mu_e^2 + 0.78\mu_e + 0.114 \qquad (22)\\ \epsilon_x = &-8.86\times10^{-5}\epsilon_e^5 + 2.43\times10^{-4}\epsilon_e^4 \\ &+ 9.39\times10^{-3}\epsilon_e^3 \\ &- 0.034\epsilon_e^2 + 1.18\epsilon_e - 0.36. \qquad (23)\end{aligned}$$

The equations presented in (22) and (23) are not universal equations and are dependent on the geometrical parameters of the strip line fixture. We have performed a comprehensive numerical study to investigate the dependence of the derived equations on different geometrical and electrical specifications of the designed strip line fixture. Our study shows that the results of the extracted μ and ϵ are independent of each other. This implies that, for a specific value of permeability, changing the permittivity does not affect the extracted value of permeability and vise versa. In addition our study shows that the extracted μ and ϵ are independent of the value of the constitutive parameters in the propagation direction, μ_z and ϵ_z. On the other hand, the extracted μ and ϵ depend on the value of constitutive parameters on the cross section of the strip line fixture, μ_x and ϵ_y, and on the geometrical parameters of the strip line, W and h. Since W, h, $\mu_x = 1$ and $\epsilon_y = \epsilon_d$ are known, they all can be included in the numerical simulation to update the fitting formulas (22) and (23) for any strip line fixture.

When deriving the fitting formulas of (22) and (23), the simulation results for a homogeneous sample are used. Since small unit cells constitute the metamaterial samples, their inhomogeneity is unavoidable; however, what of interest here is the macroscopic properties of metamaterial structure which are the average values of μ and ϵ [1]–[5]. Since the size of the unit cells is much smaller than the wavelength, it is expected that the geometry of the unit cell does not change the non-dominant field effects. Therefore, although the fitting formulas of (22) and (23) are derived using a homogeneous sample, the formulas are expected to give a reasonable accuracy when used for the effective permittivity and permeability of metamaterials with different geometries. The good accuracy illustrated in the next section for experimental characterization of metamaterials with fractal Hilbert geometry validates this conclusion.

It should be noted that the fitting formulas of (22), (23) were derived based on the special anisotropic case for metamaterials as illustrated in (20), (21). In this type of anisotropy, the values of μ_x and ϵ_y have been assumed to be equal to those of the host dielectric on which the metamaterial structure is fabricated (which are known frequency-independent constants). This assumption is valid for most metamaterial structures fabricated by stacking planar printed circuit boards to provide three-dimensional substrates. For the three-dimensional isotropic metamaterial structures which provide the same frequency-dependent parameters in all directions (reported in earlier works such as [19], [20]), the stripline method reported here is expected to work. However, if a three-dimensional metamaterial is designed in such a way that provides frequency-dependent μ_x and ϵ_y but with different values from μ_y and ϵ_x, then the fitting method reported here will not be suitable. The values of the constitutive parameters in the propagation direction, μ_z and ϵ_z, however, do not affect the fitting formulas of (22), (23). Therefore, it is of no consequence if they are assumed to be constant or frequency dependent. As shown in the section on numerical and experimental validation, despite ϵ_z being a frequency-dependent parameter, the fitting method results in a good accuracy.

To verify the accuracy of the proposed fitting solution, we consider an anisotropic sample with the constitutive parameters shown in Fig. 3. The parameters shown in Fig. 3 are selected as μ_y, and $\epsilon_x = \epsilon_z$. The extracted results before and after applying the fitting formulas are shown in Figs. 8–11, and compared with the actual data. As shown in these figures, after applying the fitting solution, the extracted parameters have acceptable agreement with the actual data.

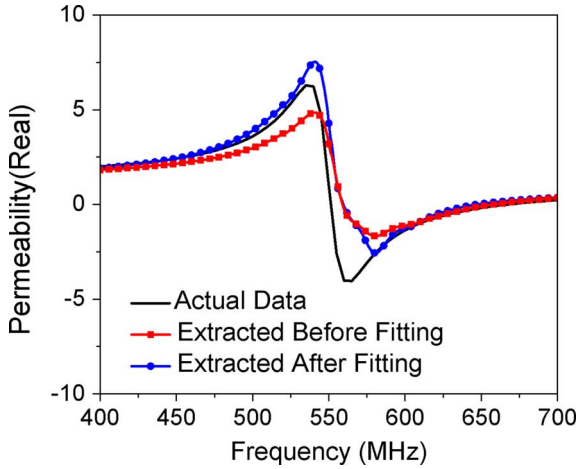

Fig. 8. Results of simulation for anisotropic sample. Real part of extracted permeability before and after fitting is plotted and compared with the actual data.

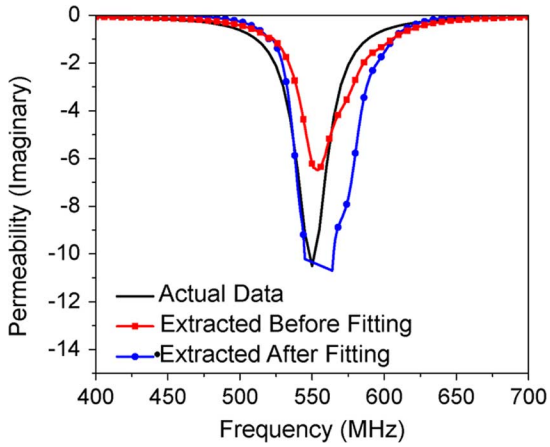

Fig. 9. Results of simulation for anisotropic sample. Imaginary part of extracted permeability before and after fitting is plotted and compared with the actual data.

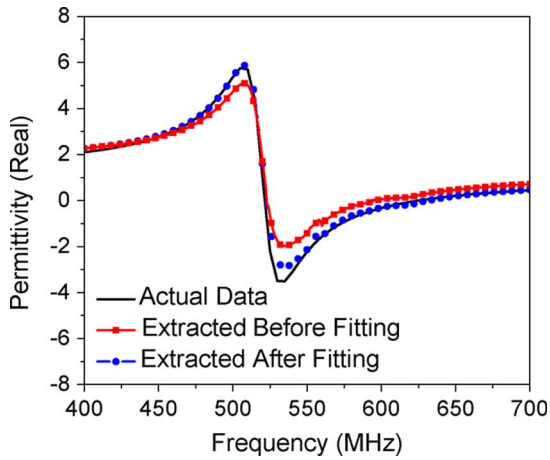

Fig. 10. Results of simulation for anisotropic sample. Real part of extracted permittivity before and after fitting is plotted and compared with the actual data.

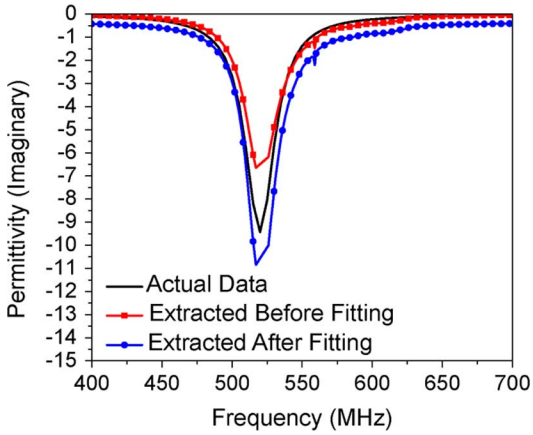

Fig. 11. Results of simulation for anisotropic sample. Imaginary part of extracted permittivity before and after fitting is plotted and compared with the actual data.

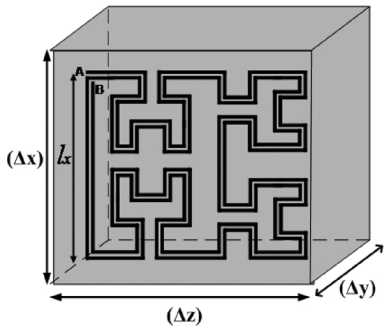

Fig. 12. Fractal Hilbert3 inclusion used for constructing magnetic metamaterial. $l_x = 8$ mm, $\Delta y = 1.57$ mm, $\Delta x = \Delta z = 11$ mm.

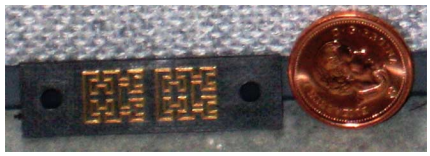

Fig. 13. A single strip containing 2 unit cells of inclusions fabricated using printed circuit board technology.

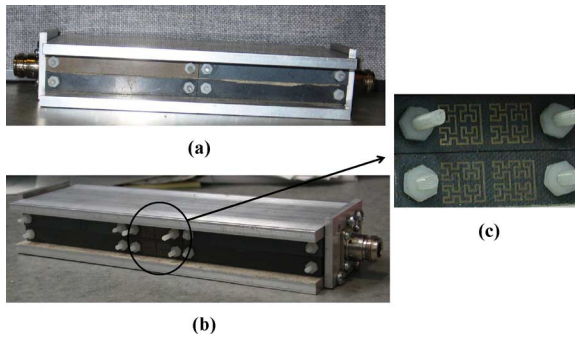

Fig. 14. The fabricated strip line fixtures. (a) without the metamaterial sample (this fixture is used as a reference), (b) with the metamaterial sample to be measured.

IV. Experimental Validation Using Fractal Hilbert3 Inclusions

The accuracy of the proposed method is tested by experimentally characterizing an anisotropic magnetic metamaterial. A metamaterial structure based on Fractal Hilbert3 inclusions is designed to achieve a magnetic response with negative permeability [17], [42]. The unit cell of the structure is shown in Fig. 12. The inclusion consists of a conducting trace having a width of $w = 0.110$ mm and separation between the traces is $s = 0.110$ mm. This metamaterial was fabricated and characterized using the strip line fixture method.

Using printed circuit technology, strips with 2 unit cells of the Fractal Hilbert3 inclusions were fabricated as shown in Fig. 13. The substrate material is Rogers RT/duroid 5880 with $\epsilon_r = 2.2$ and $\tan\delta = 0.0009$. A three-dimensional metamaterial substrate was assembled by stacking 33 of the fabricated strips in the y direction. Due to the thickness of the metal strips and imperfection in the procedure used to stack the strips, an average air gap of 50 μm develops between the strips. The air gap while unavoidable in the fabrication process is nevertheless measurable. Therefore the effect of the air gap can be easily included in the design. The fabricated metamaterial substrate has dimensions of 5.5 cm, 4 cm, and 1.1 cm in the y, z, and x directions, respectively. The strip line fixture has dimensions of $l = 22$ cm, $t = 4$ cm, $h = 22$ mm, $W = 18$ mm. (see Fig. 1) The fixtures used for characterization of the metamaterial substrate are shown in Fig. 14(a), (b). The fixture shown in Fig. 14(a) is used to measure the properties of the strip line without the metamaterial sample. These measurements are used to determine the phase reference plane for the measurement results of the fixture with the meetamaterial sample. Using a vector network analyzer, the S-parameters of the fixture shown in Fig. 14(a) were measured. These parameters are presented in Figs. 15 and 16. The fabricated strip line fixture has the return loss of less than -20 dB and insertion loss better than 0.1 dB when the metamaterial sample is not present. Therefore, the transitions between the connectors and the strip line provides sufficient accuracy needed for extraction of constitutive parameters of the metamaterial substrate. Fig. 16 shows the phase of the measured S_{21} along with the phase shift expected in the case of a transmission line with a length of 20 cm. These results show that the strip line without the sample can be modeled as a transmission line with a physical length of 20 cm. The actual length of the strip line fixture without the metamaterial sample is 18 cm. The

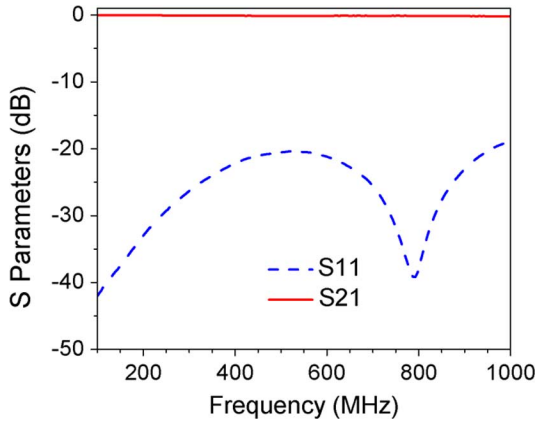

Fig. 15. Magnitude of the measured S parameters of the reference fixture (see Fig. 14(a)).

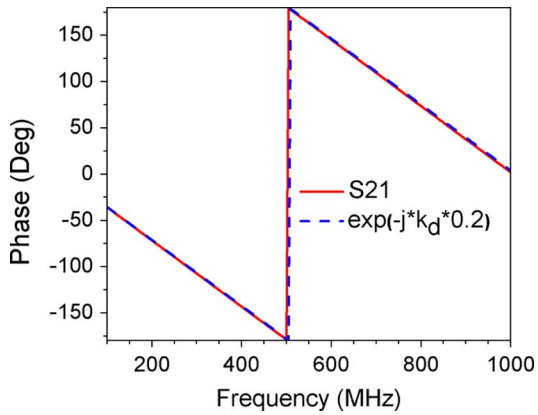

Fig. 16. Phase of the measured S21 of the reference fixture (see Fig. 14(a)).

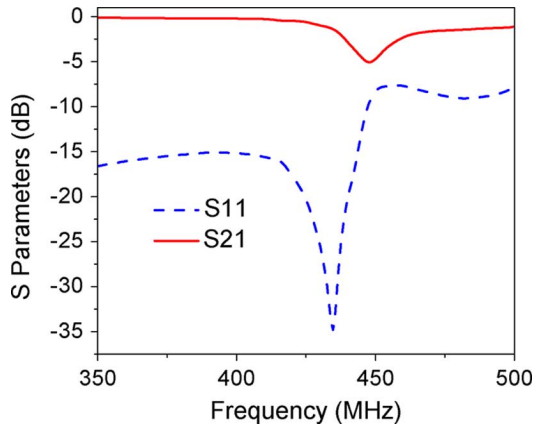

Fig. 17. Magnitude of the measured S parameters of the fixture with the metamaterial sample (see Fig. 14(b)).

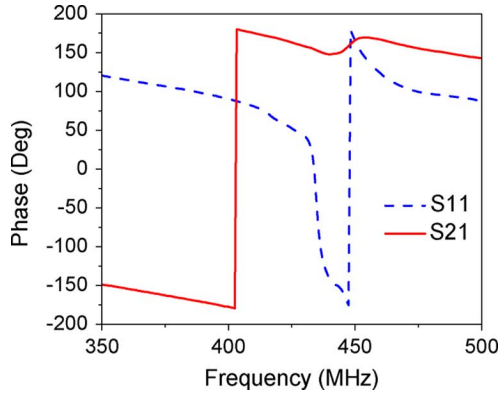

Fig. 18. Phase of the measured S parameters of the fixture with the metamaterial sample (see Fig. 14(b)).

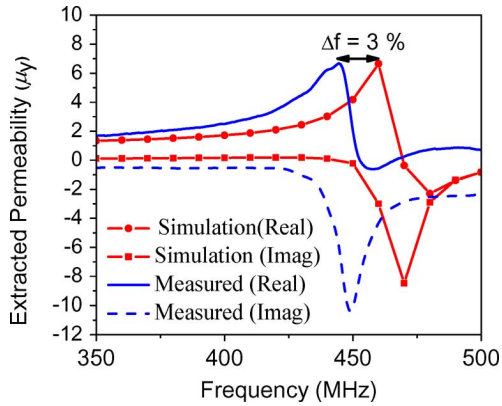

Fig. 19. The Extracted measured permeability after fitting (using (22)) is compared with numerical simulation results.

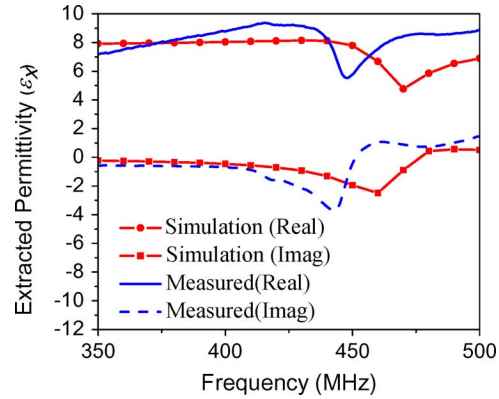

Fig. 20. The Extracted measured permittivity after fitting (using (23)) is compared with numerical simulation results.

extra phase delay is provided by the N-type connectors. The data shown in Fig. 16 is used as a reference to determine the phase reference plane for the measurement results when the metamaterial sample is placed in the middle of the strip line. Next, the S-parameters of the fixture with the metamaterial sample as shown in Fig. 14(b) is measured. The magnitude, and phase of the measured S-parameters are presented in Figs. 17 and 18, respectively.

Using the measured S-parameters and the extraction method explained in Section II along with the fitting formulas in (22) and (23), the constitutive parameters of the metamaterial sample are extracted as shown in Figs. 19 and 20. In this extraction, the phase of the measured S_{21} of the reference fixture (shown in Fig. 16) is subtracted from the phase of the measured S_{11} and S_{21} after inserting the metamaterial sample. The subtraction is necessary to eliminate the phase delay due to the two transmission lines before and after the sample. The results are compared with the constitutive parameters extracted numerically.

The numerical results are obtained using Ansoft HFSS10, and the numerical setup reported in [17]. In the numerical setup, a unit cell of the artificial material combined with periodic boundary conditions are used to mimic an infinite slab of artificial materials. For numerically extraction of constitutive parameters, plane wave analysis is used, and parameters are extracted from the reflected and transmitted waves from the unit cell [17]. The 50 μm air gap was also included in the simulation. As shown in Figs. 19 and 20, good agreement is observed between the simulation and measurement results. It should be noted that in the numerical analysis periodic boundary conditions are used to mimic an infinite number of unit cells. However, in practice we can realize only finite number of unit cells. For example in the setup used in this work (see Fig. 14), the fabricated substrate contains 33 unit cells of inclusions in the y direction, and only *two* unit cells in the x direction. Increasing the number of unit cells provides higher homogeneity in the fabricated substrate, thus expected to yield better agreement with measurements. However; on the other hand, in a wide class of applications such as antenna miniaturization, only few unit cells is used in the x direction to avoid high profile substrates [43], [44].

V. Conclusion

This work presented a new method for metamaterial characterization. The sample under test is used as the substrate of a strip line structure and the permittivity and permeability of the sample are extracted from the measured S-parameters. The method is inexpensive, easy to build and does not require a large sample. The method and the extraction theory are verified numerically for isotropic single and double negative materials. The method is also applied to the characterization of anisotropic metamaterials by employing a fitting function that compensates for the anisotropic behavior of the sample under test. To validate the method experimentally, an anisotropic sample is designed and fabricated. The strip line structure extracted the permittivity and permeability of the fabricated sample with less then 3% shift in the resonance frequency in comparison with the numerically extracted parameters.

References

[1] V. G. Veselago, "The electrodynamics of substances with simultaneously negative values of ϵ and μ," *Soviet Phys. Usp.*, vol. 10, pp. 509–514, 1968.

[2] N. Engheta and R. W. Z. , *Metamaterials: Physics and Engineering Explorations*. Hoboken-Pistacatway, NJ: Wiley-IEEE Press, 2006.

[3] G. V. Eleftheriades, *Negative-Refraction Metamaterials*. Hoboken, NJ: Wiley, 2006.

[4] A. Kabiri, L. Yousefi, and O. M. Ramahi, "On the fundamental limitations of artificial magnetic materials," *IEEE Trans. Antennas Propag.*, vol. 58, no. 7, pp. 2345–2353, Jul. 2010.

[5] J. B. Pendry, "Negative refraction makes perfect lens," *Phys. Rev. Lett.*, vol. 85, pp. 3966–3969, Oct. 2000.

[6] J. B. Pendry, A. J. Holden, D. J. Robbins, and W. J. Stewart, "Low frequency plasmons in thin-wire structures," *J. Phys.: Condens. Matter*, vol. 10, pp. 4785–4809, June 1998.

[7] J. B. Pendry, A. J. Holden, D. J. Robbins, and W. J. Stewart, "Magnetism from conductors and enhanced nonlinear phenomena," *IEEE Trans. Microwave Theory Tech.*, vol. 47, pp. 2075–2084, Nov. 1999.

[8] D. Schurig, J. J. Mock, B. J. Justice, S. A. Cummer, J. B. Pendry, A. F. Starr, and D. R. Smith, "Metamaterial electromagnetic cloak at microwave frequencies," *Science*, vol. 314, pp. 977–980, Nov. 2006.

[9] R. W. Ziolkowski and A. D. Kipple, "Application of double negative materials to increase the power radiated by electrically small antennas," *IEEE Trans. Antennas Propag.*, vol. 51, no. 10, pp. 2626–2640, Oct. 2003.

[10] L. Yousefi, B. Mohajer-Iravani, and O. Ramahi, "Enhanced bandwidth artificial magnetic ground plane for low-profile antennas," *IEEE Antennas Wireless Propag. Lett.*, vol. 6, pp. 289–292, 2007.

[11] Y. Lee, W. Park, J. Yeo, and R. Mittra, "Directivity enhancement of printed antennas using a class of metamaterial superstrates," *Electromagnetics*, vol. 26, pp. 203–218, Apr. 2006.

[12] H. Attia, L. Yousefi, M. Bait-Suwailam, M. Boybay, and O. M. Ramahi, "Enhanced-gain microstrip antenna using engineered magnetic superstrates," *IEEE Antennas Wireless Propag. Lett.*, vol. 8, pp. 1198–1201, 2009.

[13] M. S. Boybay and O. M. Ramahi, "Near-field probes using double and single negative media," *Phys. Rev. E*, vol. 79, p. 016602, Jan. 2009.

[14] C. Holloway, D. Love, E. Kuester, A. Salandrino, and N. Engheta, "Subwavelength resonators: On the use of metafilms to overcome the $\lambda/2$ size limit," *IET Microw. Antennas Propag.*, vol. 2, no. 2, pp. 120–129, Feb. 2008.

[15] R. Marques, F. Medina, and R. Rafii-El-Idrissi, "Role of bianisotropy in negative permeability and left-handed metamaterials," *Phys. Rev. B*, vol. 65, p. 144440, Apr. 2002.

[16] A. Erentok, P. Luljak, and R. Ziolkowski, "Characterization of a volumetric metamaterial realization of an artificial magnetic conductor for antenna applications," *IEEE Trans. Antennas Propag.*, vol. 53, no. 1, pp. 160–172, Jan. 2005.

[17] L. Yousefi and O. Ramahi, "Artificial magnetic materials using fractal Hilbert curves," *IEEE Trans. Antennas Propag.*, vol. 58, no. 8, pp. 2614–2622, Aug. 2010.

[18] A. Erentok, R. W. Ziolkowski, J. A. Nielsen, R. B. Greegor, C. G. Parazzoli, M. H. Tanielian, S. A. Cummer, B.-I. Popa, T. Hand, D. C. Vier, and S. Schultz, "Low frequency lumped element-based negative index metamaterial," *Appl. Phys. Lett.*, vol. 91, no. 18, p. 184104, Nov. 2007.

[19] E. Verney, B. Sauviac, and C. R. Simovski, "Isotropic metamaterial electromagnetic lens," *Phys. Lett. A*, vol. 331, no. 3–4, pp. 244–247, 2004.

[20] J. D. Baena, L. Jelinek, and R. Marqués, "Towards a systematic design of isotropic bulk magnetic metamaterials using the cubic point groups of symmetry," *Phys. Rev. B*, vol. 76, no. 24, p. 245115, Dec. 2007.

[21] L. Chen, C. K. Ong, and B. T. G. Tan, "Cavity perturbation technique for the measurement of permittivity tensor of uniaxially anisotropic dielectrics," *IEEE Trans. Instrum. Meas*, vol. 48, pp. 1023–1030, Dec. 1999.

[22] K. Buell and K. Sarabandi, "A method for characterizing complex permittivity and permeability of meta-materials," in *Proc. IEEE Antennas and Propagation Society Int. Symp.*, Jun. 2002, vol. 2, pp. 408–411.

[23] R. B. Greegor, C. G. Parazzoli, K. Li, B. E. C. Koltenbah, and M. Tanielian, "Experimental determination and numerical simulation of the properties of negative index of refraction materials," *Opt. Expr.*, vol. 11, pp. 688–695, Apr. 2003.

[24] A. F. Starr, P. M. Rye, D. R. Smith, and S. Nemat-Nasser, "Fabrication and characterization of a negative-refractive-index composite metamaterial," *Phys. Rev. B*, vol. 70, p. 113102, Sep. 2004.

[25] D. R. Smith, D. Schurig, and J. J. Mock, "Characterization of a planar artificial magnetic metamaterial surface," *Phys. Rev. E*, vol. 74, p. 036604, Sep. 2006.

[26] N. J. Damascos, R. B. Mack, A. L. Maffett, W. Parmon, and P. L. E. Uslenghi, "The inverse problem for biaxial materials," *IEEE Trans. Microw. Theory Tech.*, vol. 32, no. 4, pp. 400–405, Apr. 1984.

[27] H. Chen, J. Zhang, Y. Bai, Y. Luo, L. Ran, Q. Jiang, and J. A. Kong, "Experimental retrieval of the effective parameters of metamaterials based on a waveguide method," *Opt. Expr.*, vol. 14, no. 26, pp. 12 944–12 949, Dec. 2006.

[28] L. Yousefi, H. Attia, and O. M. Ramahi, "Broadband experimental characterization of artificial magnetic materials based on a microstrip line method," *J. Progr. Electromagn. Res. (PIER)*, vol. 90, pp. 1–13, Feb. 2009.

[29] L. F. Chen, C. K. Ong, C. P. Neo, V. V. Varadan, and V. K. Varadan, *Microwave Electronics Measurement and Materials Characterization*. Hoboken, NJ: Wiley, 2004.

[30] M. S. Boybay, S. Kim, and O. M. Ramahi, "Negative material characterization using microstrip line structures," in *Proc. IEEE AP-S Int. Symp. Antennas Propagation*, Jul. 2010, vol. 1B, pp. 1–4.

[31] A. Erentok, R. W. Ziolkowski, J. A. Nielsen, R. B. Greegor, C. G. Parazzoli, M. H. Tanielian, S. A. Cummer, B.-I. Popa, T. Hand, D. C. Vier, and S. Schultz, "Low frequency lumped element-based negative index metamaterial," *Appl. Phys. Lett.*, vol. 91, pp. 1 841 041–1 841 043, Nov. 2007.
[32] J. Baker-Jarvis, E. J. Vanzura, and W. A. Kissick, "Improved technique for determining complex permittivity with the transmission/reflection method," *IEEE Trans. Microwave Theory Tech.*, vol. 38, no. 8, pp. 1096–1103, Aug. 1990.
[33] P. Queffelec, P. Gelin, J. Gieraltowski, and J. Loaec, "A microstrip device for the broad band simultaneous measurement of complex permeability and permittivity," *IEEE Trans. Magn.*, vol. 30, no. 2, pp. 224–231, Mar. 1994.
[34] Y. Heping, K. Virga, and J. Prince, "Dielectric constant and loss tangent measurement using a stripline fixture," *IEEE Trans. Adv. Packag.*, vol. 21, pp. 441–446, Nov. 1999.
[35] J. Hinojosa, L. Faucon, P. Queffelec, and F. Huret, "S-parameter broadband measurements of microstrip lines and extraction of the substrate intrinsic properties," *Microw. Opt. Technol. Lett.*, vol. 30, no. 1, pp. 65–69, Jul. 2001.
[36] V. Bekker, K. Seemann, and H. Leiste, "A new strip line broad-band measurement evaluation for determining the complex permeability of thin ferromagnetic films," *J. Magnetism Magn. Mater.*, vol. 270, no. 3, pp. 327–332, 2004.
[37] W. Davis, C. Bunting, and S. Bucca, "Measurement and analysis for stripline material parameters using network analyzers," in *Proc. Instrumentation and Measurement Technology Conf. IMTC-91.*, May 1991, pp. 568–572.
[38] W. Davis, C. Bunting, and S. Bucca, "Measurement and analysis for stripline material parameters using network analyzers," *IEEE Trans. Instrum. Meas.*, vol. 41, no. 2, pp. 286–290, Apr. 1992.
[39] J. Hinojosa, "Permittivity characterization from open-end microstrip line measurements," *Microw. Opt. Technol. Lett.*, vol. 49, no. 6, pp. 1371–1374, 2007.
[40] D. M. Pozar, *Microwave Engineering*, 2nd ed. New York: Wiley, 1998.
[41] R. W. Ziolkowski, "Design, fabrication, and testing of double negative metamaterials," *IEEE Trans. Antennas Propag.*, vol. 51, no. 7, pp. 1516–1529, Jul. 2003.
[42] L. Yousefi and O. M. Ramahi, "Miniaturised antennas using artificial magnetic materials with fractal Hilbert inclusions," *Electron. Lett.*, vol. 46, no. 12, pp. 816–817, 2010.
[43] K. Buell, H. Mosallaei, and K. Sarabandi, "A substrate for small patch antennas providing tunable miniaturization factors," *IEEE Trans. Microw. Theory Tech.*, vol. 54, pp. 135–146, Jan. 2006.
[44] P. M. T. Ikonen, S. I. Maslovski, C. R. Simovski, and S. A. Tretyakov, "On artificial magnetodielectric loading for improving the impedance bandwidth properties of microstrip antennas," *IEEE Trans. Antenna Propag.*, vol. 54, pp. 1654–1662, Jun. 2006.

Leila Yousefi (M'09) was born in Isfahan, Iran, in 1978. She received the B.Sc. and M.Sc. degrees in electrical engineering from Sharif University of Technology, Tehran, Iran, in 2000, and 2003 respectively, and the Ph.D. degree in electrical engineering from University of Waterloo, Waterloo, ON, Canada, in 2009.

Currently she is working as a Postdoctoral Fellow at the University of Waterloo. Her research interests include metamaterials, miniaturized antennas, electromagnetic bandgap structures, and MIMO systems.

Muhammed Said Boybay (S'07–M'09) received the B.S. degree in electrical and electronics engineering from Bilkent University, Turkey, in 2004 and the Ph.D. degree in electrical and computer engineering from the University of Waterloo, Waterloo, ON, Canada, Canada, in 2009.

From 2004 to 2009, he was a Research and Teaching Assistant in the Mechanical and Mechatronics Engineering, and Electrical and Computer Engineering Departments, University of Waterloo. Currently, he is a Postdoctoral Fellow in the Department of Electrical and Computer Engineering, University of Waterloo. His research interests include double and single negative materials, near field imaging, electrically small resonators, electromagnetic bandgap structures and EMI/EMC applications.

Omar M. Ramahi (F'09) was born in Jerusalem, Palestine. He received the B.S. degrees in mathematics and electrical and computer engineering (*summa cum laude*) from Oregon State University, Corvallis, and the M.S. and Ph.D. in electrical and computer engineering from the University of Illinois at Urbana-Champaign.

He held a visiting fellowship position at the University of Illinois at Urbana-Champaign and then worked at Digital Equipment Corporation (presently, HP), where he was a member of the Alpha Server Product Development Group. In 2000, he joined the faculty of the James Clark School of Engineering, University of Maryland at College Park, as an Assistant Professor and later as a tenured Associate Professor. At Maryland, he was also a faculty member of the CALCE Electronic Products and Systems Center. Presently, he is a Professor in the Electrical and Computer Engineering Department and holds the NSERC/RIM Industrial Research Associate Chair, University of Waterloo, Waterloo, ON, Canada. He holds cross appointments with the Department of Mechanical and Mechatronics Engineering and the Department of Physics and Astronomy. He served as a consultant to several companies and was a co-founder of EMS-PLUS, LLC and Applied Electromagnetic Technology, LLC. He has authored and coauthored over 240 journal and conference papers. He is a coauthor of the book *EMI/EMC Computational Modeling Handbook,* (Springer-Verlag, 2001).

Dr. Ramahi presently serves as an Associate Editor for the IEEE TRANSACTIONS ON ADVANCED PACKAGING and as the IEEE EMC Society Distinguished Lecturer.